Accepted Manuscript

Antitumor activity of pyrrolizines and their Cu(II) complexes: Design, synthesis and cytotoxic screening with potential apoptosis-inducing activity

Ahmed M. Gouda, Hoda A. El-Ghamry, Tahani M. Bawazeer, Thoraya A. Farghaly, Ashraf N. Abdalla, Akhmed Aslam

PII: S0223-5234(18)30009-6

DOI: 10.1016/j.ejmech.2018.01.009

Reference: EJMECH 10086

To appear in: *European Journal of Medicinal Chemistry*

Received Date: 23 November 2017

Revised Date: 1 January 2018

Accepted Date: 4 January 2018

Please cite this article as: A.M. Gouda, H.A. El-Ghamry, T.M. Bawazeer, T.A. Farghaly, A.N. Abdalla, A. Aslam, Antitumor activity of pyrrolizines and their Cu(II) complexes: Design, synthesis and cytotoxic screening with potential apoptosis-inducing activity, *European Journal of Medicinal Chemistry* (2018), doi: 10.1016/j.ejmech.2018.01.009.

Graphical abstract

Antitumor Activity of Pyrrolizines and their Cu(II) Complexes: Design, Synthesis and Cytotoxic Screening with potential Apoptosis-Inducing Activity

Ahmed M. Gouda, Hoda A. El-Ghamry, Tahani M. Bawazeer, Thoraya A. Farghaly*, Ashraf N. Abdalla, Akhmed Aslam

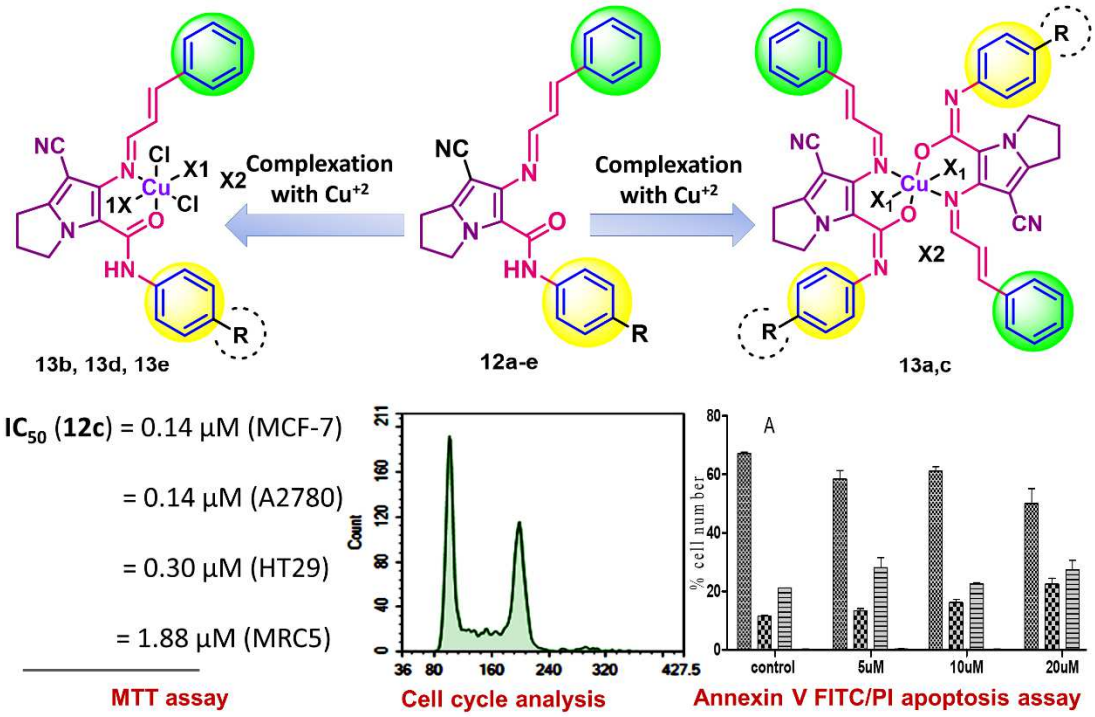

Antitumor Activity of Pyrrolizines and their Cu(II) Complexes: Design, Synthesis and Cytotoxic Screening with potential Apoptosis-Inducing Activity

Ahmed M. Gouda[1,2], Hoda A. El-Ghamry[3,4], Tahani M. Bawazeer[4,5], Thoraya A. Farghaly[6]*, Ashraf N. Abdalla[7,8], Akhmed Aslam[9]

[1]Medicinal chemistry department, Faculty of pharmacy, Beni-Suef University, Beni-Suef 62514, Egypt; [2]Department of Pharmaceutical Chemistry, Faculty of Pharmacy, Umm Al-Qura University, Makkah 21955, Saudi Arabia; [3]Chemistry Department, Faculty of Science, Tanta University, Tanta, Egypt; [4]ChemistryDepartment, Faculty of Applied Science, Umm Al–Qura University, Makkah, Saudi Arabia; [5]Medical Applications of Nanobiotechnology Research Group, King Fahad Medical Research Center, King Abdulaziz University, Jeddah, Saudi Arabia; [6]Department of Chemistry Faculty of Science, Cairo University, Giza, Egypt; [7]Department of Pharmacology and Toxicology, Faculty of Pharmacy, Umm Al-Qura University, Makkah 21955, Saudi Arabia; [8]Departmentof Pharmacology, Medicinal and Aromatic plants research institute, National center for research, Khartoum 2404, Sudan; [9]Department of Laboratory Medicine, Faculty of Applied Medical Sciences, Umm Al-Qura University, Makkah 21955, Saudi Arabia.

***Corresponding author email address:** thoraya-f@hotmail.com

---

Abstract:

Two novel series including Schiff bases of the pyrrolizine-5-carboxamides and their Cu(II) complexes were designed, synthesized and analyzed using spectral and analytical techniques. The analytical results indicated the formation of the complexes in 1:1 or 1:2 (Metal:Ligand) ratio. The geometry around the Cu centers was confirmed to be tetrahedral or octahedral. The cytotoxic activity of the new compounds was evaluated using MCF-7 (human breast adenocarcinoma), A2780 (human ovary adenocarcinoma) and HT29 (human colon adenocarcinoma), in addition to MRC5 (normal human fetal lung fibroblast)cells using the MTT cytotoxicity assay. The Schiff base **12c** and the Cu complex **13b** were the most active in the two series with IC_{50} values in the range of 0.14-2.54 µM against the three cell lines. Also, the Cu complex **13e** showed excellent activity against HT29 with IC_{50} = 0.05µM. 7-Cyano-*N*-(4-methoxyphenyl)-6-((3-phenylallylidene) amino)-2,3-dihydro-1*H*-pyrrolizine-5-carboxamide **(12c)** showed high selectivity (6-13 folds) for cancerous cells over normal cells; and it induced marginal increases in the G1 and S phases of MCF-7 cells during cell cycle analysis, while

compound **13b** increased the MCF-7 Sub-G1 proapoptotic population, and blocked cells in the G2-M phase in a dose dependent manner. The annexin V apoptosis assay revealed the ability of compounds **12c** and **13b** to increase the early apoptotic MCF-7 cell populations two and three fold, respectively. Furthermore, these findings were supported by data showing that the two compounds (**12c** and **13b**) elicit cytotoxic activity. Taken together, the data presented in this study warrants further *in vitro* and *in vivo* investigations.

Keywords: Pyrrolizine; Cinnamaldehyde; Schiff bases; Copper complexes; Cytotoxicity; Cell cycle; Apoptosis

1. Introduction

Cancer is amongst the terrifying diseases occurring worldwide, being the second cause of illness caused death, and accounting for one-sixth of the global deaths in 2015 [1]. Currently, the evolution of resistance to some of the clinically available anticancer drugs has been reported [2,3]. These factors encourage research in this fast-moving area to discover and develop new potent and selective anticancer agents. Induction of apoptosis has a crucial role in development and treatment of cancer [4]. The complicated signaling pathway of apoptosis involves many regulatory and inhibitory proteins and pathways. Large numbers of anticancer agents target these proteins and exert their anticancer action through induction of apoptosis in cancer cells [5].

Of these potential anticancer agents, several pyrrolizines bearing diarylfragments (Fig. 1) have been developed, that have displayed diverse biological activities [6-8]. Licofelone **1** displayed potent anticancer activity against breast, colon and prostate cancers [9-11]. Mechanistic studies revealed the ability of licofelone **1** to activate caspase 3/9 and trigger apoptosis through a mitochondrial pathway [10]. Compound **2** (Fig. 1) was also reported to induce a potent anticancer activity against MCF-7 and PC-3 cancer cell lines [12]. Replacement of the 4-nitrophenyl moiety in compound **2** with the bulky naphthalenyl generated compound **3,** which displayed potent anticancer activity and exhibited selective inhibition of cyclooxygenase 2 (COX-2), activation of caspase3/7 and induction apoptosis [13].

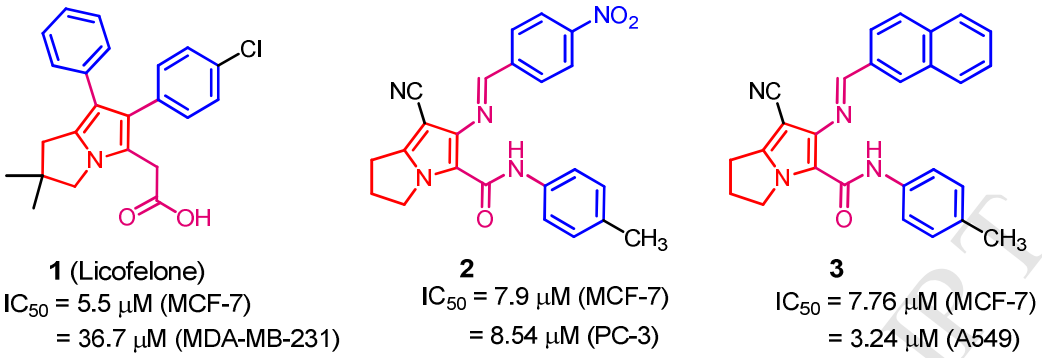

Fig. 1. Representative pyrrolizineswith anticancer activity against diverse cancer cell lines.

On the other hand, several small molecules of the cinnamaldehyde scaffold have been reported as apoptosis inducing anticancer agents (Fig. 2). Cinnamaldehyde compound **4** inhibited the proliferation of several types of cancer cells and induced apoptosis through the activation of reactive oxygen species (ROS) in HL-60 leukemia cells [14]. Moreover, compound **5** (CB403) inhibited the growth of ten types of cancer cell lines with GI_{50} in the range of 1.61 to 10.77 μg/mL. This compound also initiated the cell cycle arrest of MCF-7 cells in the G2-M phase [15]. In addition, compound **6** was also to arrest the cell cycle of the cis-platin-resistant ovarian A2780cis cells in the G2-M phase and to induce apoptosis [16].

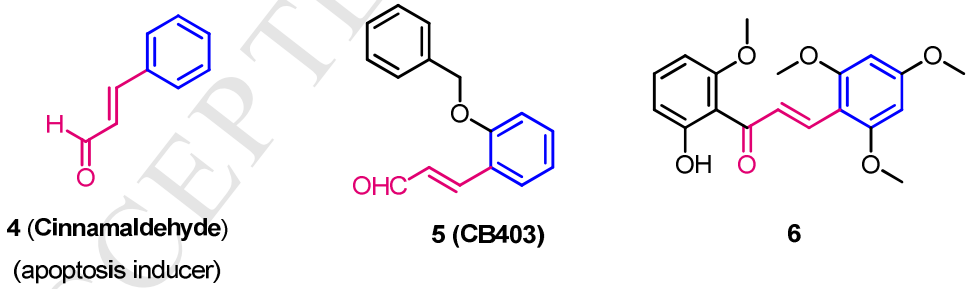

Fig. 2. Cinnamaldehyde-based anticancer compoundswith apoptosis inducing/cell cycle blocking activity.

In this study, new pyrrolizines (Fig. 3) were designed using the following design strategy, (1) Cinnamaldehyde was selected for the preparation of the new Schiff bases based on previous reports showing its apoptosis inducing anticancer activity [14-16]. (2) Scaffold A was designed as a modification of compound **2**, with elongation of the spacer between phenyl ring and the

pyrrolizine nucleus. (3) Several Cu(II) complexes with Schiff bases have displayed potent antiproliferative activities mediated by the induction of apoptosis [17-19]. Accordingly, it was of interest to design scaffold B as Cu(II) complexes with the designed Schiff bases. (4) Various substituents including electron donating (R = CH_3/OCH_3), electron withdrawing (R = Cl/Br) and the unsubstituted phenyl ring (R = H) were used to study their impact on activity.

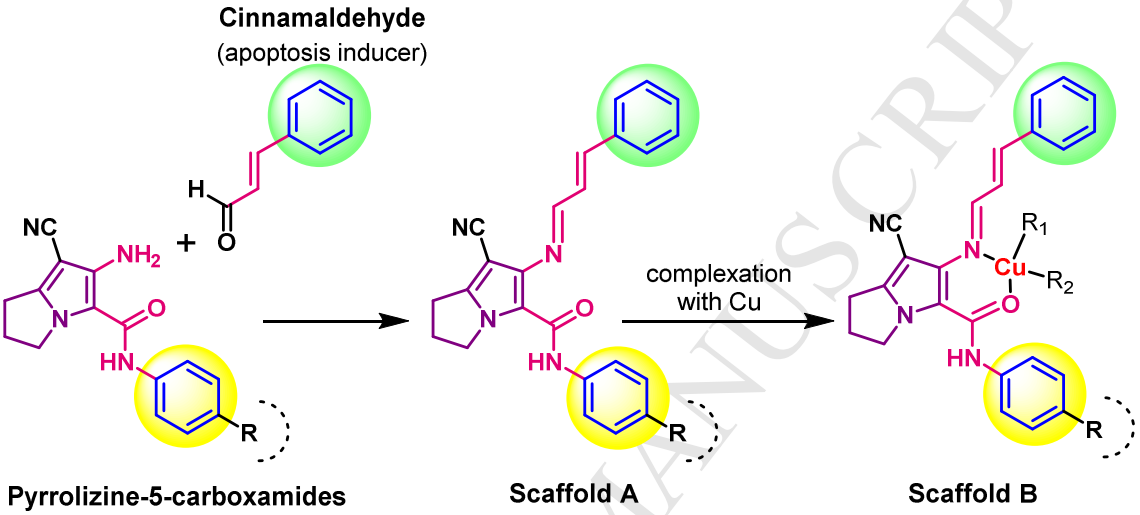

Fig. 3. Design strategies of scaffold A and B

2. Results and discussion

2.1. Chemistry

Preparation of compounds **8** [20], **10a-e** [21] and **11a-e** [22] was outlined in Scheme 1 according to the reported methods. Condensation of compounds **11a-e** with cinnamaldehyde in absolute ethanol afforded the five Schiff bases **12a-e**, Scheme 1.

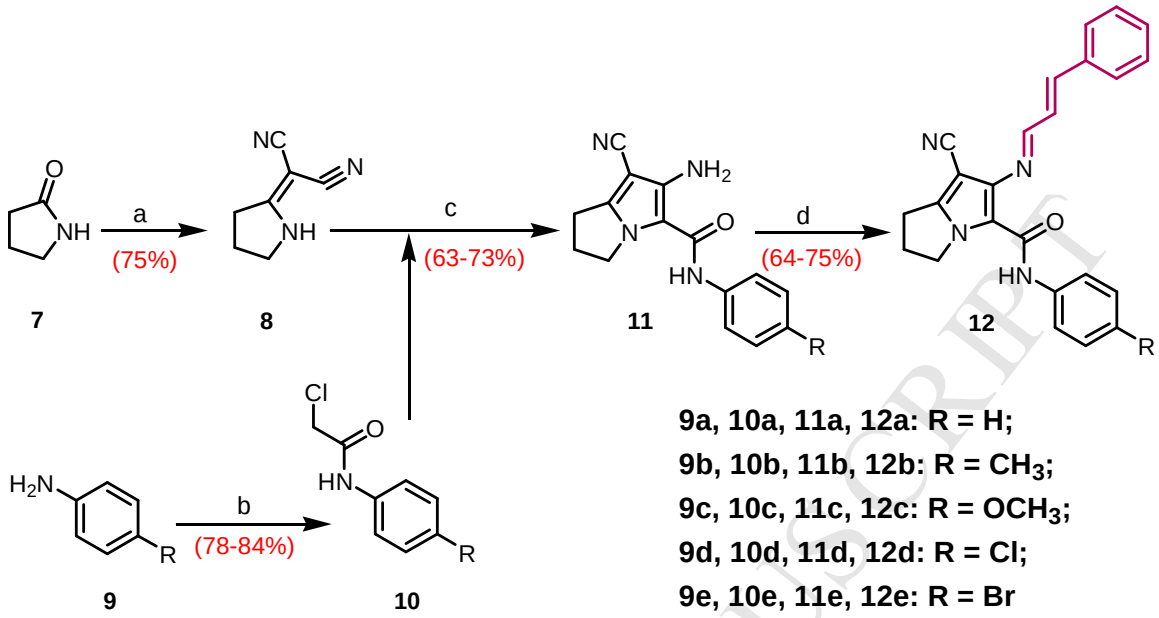

Scheme 1. Reagents and conditions: (a) $(CH_3)_2SO_4$, benzene, $CH_2(CN)_2$; (b) $ClCH_2COCl$, g. acetic acid, CH_2COONa; and (c) acetone, K_2CO_3, reflux, 24 h; (d) *trans*-cinnamaldehyde, absolute ethanol, glacial acetic acid, reflux, 6 h.

Characterization of compounds **12a-e** was done using spectral and elemental analyses. The ^{1}H-NMR of all derivatives **12a-e** revealed doublet signals at 8.85-8.91 ppm, indicating the N=CH, and another singlet signal at the range of 10.61-10.88 ppm, which disappeared on deuteration and indicated the presence of amide NHs. The ^{13}C-NMR revealed two signals at the range of 157.92-162.14 ppm, indicating the presence of N=CH and the carbonyl carbon. Mass spectra of compounds **12a-e** revealed the molecular ion peaks at m/z = 380, 394, 410, 414, and 458, respectively, with 72-100% intensity. The fragmentation patterns of compounds **12a-e** were matched with their chemical structures.

2.2. Synthesis and investigation of Cu(II) complexes

Preparation of Cu(II) chelates was performed according to Scheme 2. The ligands (**12a-e**) were reacted with $CuCl_2.2H_2O$ in a refluxing acetonitrile medium in the molar ratio 1:1 (metal: ligand) to obtain the desired Cu(II) complexes (**13a-e**), which are readily soluble in DMSO and DMF solvents. All the complexes are non-hygroscopic and stable in air for a long period of time. The elemental analyses data for Cu (II) complexes are in

agreement with the proposed molecular formulae and all metal complexes are deep brown in color.

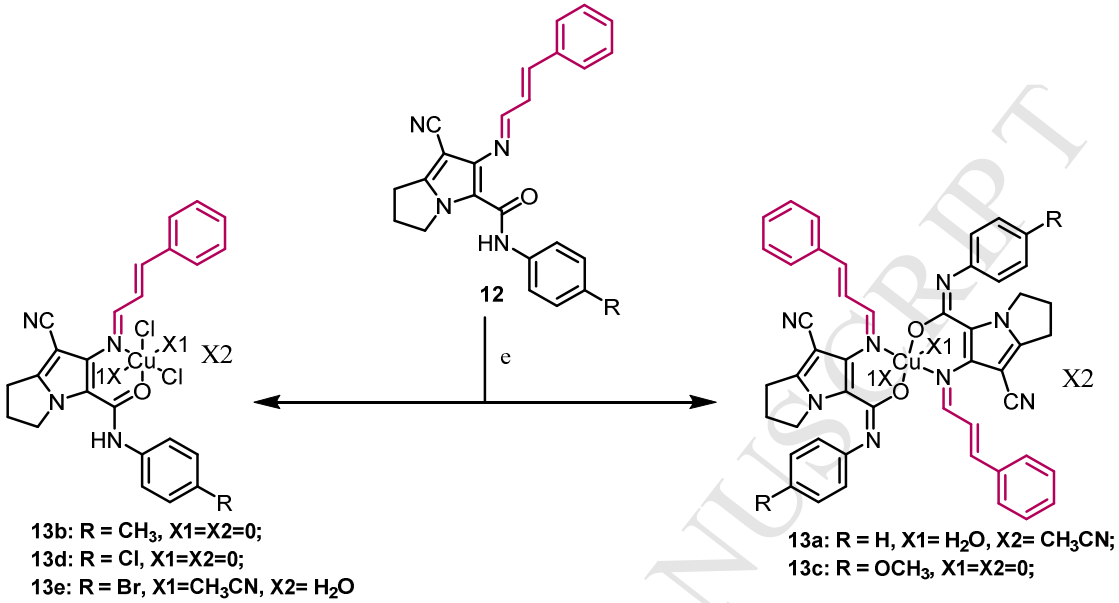

Scheme 2.Reagents and conditions: (e) $CuCl_2.2H_2O$, acetonitrile

2.2.1 Elemental analysis and molar conductance

The elemental analysis results of the metal chelates are consistent with the postulated molecular formulae and confirm the formation of 1:1 (M:L) complexes for compounds **13b**, **13d** and **13e,** and 1:2 (M:L) complexes for compounds **13a** and **13c**. The measured molar conductance values (12.20–16.8 $\Omega^{-1}cm^2$ mol^{-1}) of all chelates in 10^{-3}M DMF solvent assured their non-electrolytic type [23].

2.2.2. FT-IR spectra

In order to detect the coordination sites in the ligand that contribute in bond formation with the central metal ion, the FTIR spectra of the metal chelates are compared with that of the free ligand. There are some peaks in the ligand spectrum that guide us to understand this issue. These peaks change either in their positions and/or their intensities upon chelation. Some other peaks disappear after complexation.

In the ligands spectra, the carbonyl and azomethine stretching vibration bands appeared within the 1673-1616 & 1610-1578 cm^{-1} ranges, respectively. In the spectra of compounds **13a**

&**13c**, the carbonyl bands have disappeared revealing the involvement of this band in mesomerism (i.e. keto-amine/enol-imine structures); the mesomeric form containing –N=C-OH type of arrangement, most probably involved in the bond formation coordinating to the metal centers through deprotonated hydroxyl groups [24, 25]. This type of mesomerism was confirmed by the appearance of two C=N peaks at 1694 & 1579 cm^{-1} for compound **13a** and at 1689 & 1607 for compound **13c,** one of these two C=N bands was involved in coordination to the metal center through a nitrogen atom. Analytical results strongly supported the formation of such mesomeric structures. For compounds **13b**, **13d** & **13e**, the position of the two bands (i.e. C=O and C=N) underwent a shift in their position to higher or lower wavenumbers, proving their coordination to the metal centers. These observations are confirmed by the outcrop of non-ligand bands at 594–520 and 494-476 cm^{-1}, which were assigned to the stretching vibrations of Cu-O and Cu-N [26].

The ligand band, which was found within the 3278-3226 cm^{-1} range, was assigned to υ(NH). The shift in position of this band, in the spectra of metal chelates, is most probably due to the involvement of this group in H-bond formation with other electronegative atoms in the ligand [26]. The appearance of a broad band at 3449 and 3447 cm^{-1} in the spectra of hydrated complexes (**13a** and **13e**) are assigned to the stretching vibrations of OH of water molecules attached to the copper center.

2.2.3. Thermogravimetric analysis

Thermogravimetric analysis (TGA) of the metal chelates is a helpful tool to understand the coordination structure of the complexes [27, 28], through affording exemplary knowledge on their thermal properties, intermediate nature, and final products of their thermal decomposition stages [29]. It is essential to realize the nature and contents of water and/or other solvent molecules and also the anion groups associated with the central atoms. Subsequently, all the synthesized metal chelates were subjected to TGA. The possible pyrolysis reaction, nature of intermediates, temperature ranges, and final decomposition products, as well as the experimental and calculated percentage mass losses in each decomposition step are collected in Table S1, while the TG thermograms are illustrated in Fig. S21-25.

The metal chelates under study were found to degrade through two (compound **13d**), three (compounds **13b** & **13c**) or four (compounds **13a** & **13e**) stages of decomposition.

The thermal decomposition of compounds **13a** and **13e**, as representative examples, can be illustrated by the following schemes. For compound **13a**, the decomposition stages are:

$$[Cu(L^{12a})_2(H_2O)_2].CH_3CN \xrightarrow[-3.81\ (calcd.\ 4.55\ \%)]{23\text{-}87\ ^oC} [Cu(L^{12a})_2(H_2O)_2]$$

$$[Cu(L^{12a})_2(H_2O)_2] \xrightarrow[-4.73\ (calcd.\ 4.00\ \%)]{87\text{-}125\ ^oC} [Cu(L^{12a})_2]$$

$$[Cu(L^{12a})_2] \xrightarrow[-28.97\ (calcd.\ 28.68\ \%)]{125\text{-}326\ ^oC} \text{Intermediate 1}$$

$$\text{Intermediate 1} \xrightarrow[-54.39\ (calcd.\ 54.32\ \%)]{326\text{-}783\ ^oC} CuO$$

For compound **13e**, the decomposition stages are:

$$[CuL^{12e}\ Cl_2(CH_3CN)_2].H_2O \xrightarrow[-1.73\ (calcd.\ 2.59\ \%)]{25\text{-}95\ ^oC} [CuL^{12e}\ Cl_2(CH_3CN)_2]$$

$$[CuL^{12e}\ Cl_2(CH_3CN)_2] \xrightarrow[-17.12\ (calcd.\ 16.94\ \%)]{95\text{-}328\ ^oC} [CuL^{12e}\ Cl]$$

$$[CuL^{12e}\ Cl] \xrightarrow[-20.72\ (calcd.\ 20.37\ \%)]{328\text{-}452\ ^oC} \text{Intermediate 1}$$

$$\text{Intermediate 1} \xrightarrow[-48.91\ (calcd.\ 48.62\ \%)]{425\text{-}749\ ^oC} CuO$$

As shown previously and as indicated in Table S1, the results of thermal analysis for the complexes **13a-e** strongly confirmed their proposed molecular composition.

2.2.4. Magnetic moment, UV-visible and ESR spectroscopy

The information about geometrical structures of the metal chelates is gained from their electronic spectra and magnetic moment data.

The magnetic moment values of Cu(II) complexes **13a-e** were found to be 1.92, 1.86, 1.92, 2.01 and 2.13 B.M. for complexes **13a**, **13b**, **13c**, **13d** and **13e**, respectively, which are close to the spin only value of one unpaired electron expected for Cu(II) compounds (theoretical value is

1.72 B.M). These values indicated that the Cu(II) complexes are monomeric in nature without Cu–Cu interaction [30, 31].

UV-Vis spectra of the metal complexes were measured in DMF solution from 200 to 900 nm. Cu(II) complexes **13a** and **13e** displayed broad absorption bands centered at 16949 and 16619 cm^{-1}, respectively, assignable to $^2E_g \rightarrow {}^2T_{2g}$ transition reported for octahedral configuration [32, 33]. The spectra of complexes **13b**, **13c** and **13d**displayed broad spectral bands at 550, 578 and 548 cm^{-1}, respectively, that assigned to $^2T_2 \rightarrow {}^2E_2$ transition, which is characteristic for tetrahedral Cu(II) complexes [34]. The possibility of square planar geometry at the metal center is ruled out hence, in general, square planar complexes are known to exhibit two bands in the visible region, around 700‑712 and 533‑550 nm as previously reported [34].

Solid state ESR spectra of complexes **13a-e** (Figs. S26-30), recorded at room temperature, displayed axially symmetric g-tensor parameters with $g_{\|} > g_{\perp} > 2.0023$ ($g_{\|}$ = 2.46, 2.28, 2.179, 2.187 & 2.45; $g_{\perp}$ = 2.11, 2.028, 2.034, 2.038 & 2.107 for complexes **13a**, **13b**, **13c**, **13d** and **13e**, respectively) representing that the unpaired electron of Cu(II) ion is located in the d_{x2-y2}orbital. Such behavior is characteristic for tetrahedrally distorted [35] or octahedral stereochemistry [36]. The spin-Hamiltonian parameters of this complex were also calculated. In axial symmetry the g-values are related by the expression, $G = (g_{\|} - 2)/(g_{\perp} - 2)$, where G is the exchange interaction parameter. According to Hathaway, if the value of G is greater than 4, the exchange interaction between Cu(II) centers in the solid state is negligible, whereas when it is less than 4, a considerable exchange interaction is indicated in the solid complex [37]. G values were calculated to be within the range 4.18-10, supporting the fact that there is no copper–copper exchange interaction between the metal centers in the investigated compounds, which also supports the increased values of the magnetic moment of the metal chelates from the spin only value of the soul unpaired electron of Cu(II) centers. No hyperfine splitting was observed in the spectra.

2.3. Pharmacology

2.3.1. Cytotoxic activity

The target compounds (**12a-e** and **13a-e**) were evaluating for their cytotoxic activities against human breast MCF-7, ovarian A2780 and colon HT29 cancer cell lines using the MTT

assay [38].The cytotoxicity of compounds **12a-e** and **13a-e** against breast (MCF-7), ovarian (A2780) and colon(HT29) cancer cell lineswere expressed as half maximal inhibitory concentration (IC_{50}) values and presented in Table 1. Moreover, cytotoxicity of the most active compounds (**12c** and **13b**) was also evaluated against a normal human lung fibroblast cell line (MRC5).

In the first series **12a-e**, the MTT assay results revealed that compound **12c** exhibited the highest activity against the breast, ovarian and colon cancer cell lines, with IC_{50} values in the range of 0.14-0.30 µM. Compound **12c** was 6-13 fold more selective for the three cancer cell lines compared to MRC5 normal cells. The second and third most active compounds were **12a** and **12d** respectively. Both compounds **12a** and **12c** showed submicromolar activity against the three cancer cells, while compound **12b** showed an IC_{50}value ≤ 2 µM against MCF-7 and HT29 cells.

Table 1. Cytotoxic activity (MTT assay) of of compounds **12a-e** and **13a-e** against the three cancer cell lines (MCF7, A2780, HT29) and MRC5 normal fibroblasts. The cells were incubated for 72h, followed by 3h with MTT. The IC_{50}±SD (μM) is shown for every compound tested against each cell line.

Compound	IC_{50} (μM)			
	MCF-7	**A2780**	**HT29**	**MRC5**
12a	0.72±0.15	0.04±0.02	0.60±0.04	nt
12b	1.94±0.06	24.66±1.00	0.13±0.01	nt
12c	0.14±0.04	0.14±0.01	0.30±0.03	1.88±0.08
12d	1.46±0.24	2.97±0.32	3.71±0.81	nt
12e	0.50±0.29	3.50±0.13	7.27±1.18	nt
13a	1.27±0.19	3.62±2.28	5.31±0.13	nt
13b	0.69±0.11	0.81±0.38	2.54±0.89	0.23±0.08
13c	3.88±1.14	0.82±0.10	0.68±0.02	nt
13d	20.84±6.41	0.16±0.01	1.20±0.01	nt
13e	22.12±4.70	4.17±1.25	0.05±0.06	nt
Lapatinib	6.80± 1.20	10.40± 0.80	12.67±1.33	12.89±3.24

Cells were treated with the new compounds or vehicle for 72 h; the results were presented as mean ±SD, n = 3; nt, not tested.

The MTT assayresults of compounds **13a-e** revealed IC_{50} values in the range of 0.05-22.12 μM against the three cancer cell lines, with compound **13b** showing the highest activity (IC_{50}values in the range of 0.69-2.54 μM). Compounds **13d** and **13e** showed potent cytotoxic activity against the A2780 and HT29 cell lines, with IC_{50} values≤ 5 μM. Interestingly, compound **13b** showed less selectivity for MRC5 compared to compound **12c**. Both compounds **12c** and **13b** showed better cytotoxicity compared to lapatinib, Table 1.

2.3.2. Determination of cell cycle perturbations

Cell cycle analysis was carried out using flow cytometry by staining of DNA within cells using propidium iodide (PI). The cell cycle distribution assay of MCF-7 cells treated with compound **12c** (24 h) was doneaccording to the reported protocols [39]. The results revealed

marginal increases in the G1 and S phases, Table 2 and Fig. 3. In contrast, compound **13b** increased the MCF-7 Sub-G1 pro-apoptotic population and blocked cells in the G2-M phase in a dose dependent manner, which was at the expense of a decrease in the G1 phase (Table 3, Fig.4).

Table 2: Cell cycle analysis of compound 12c. The distribution of the different phases was analysed using the cell cycle algorithm of the Novo Express software and expressed as percentage of total gated single events.

Stage	**Concentration**			
	Control	**5 µM**	**10 µM**	**20 µM**
Sub-G1	0.31%	0.47%	0.46%	0.46%
G1	33.41%	36.41%	39.47%	37.09%
S	24.95%	27.26%	27.20%	29.27%
G2-M	35.02%	32.94%	30.81%	28.62%

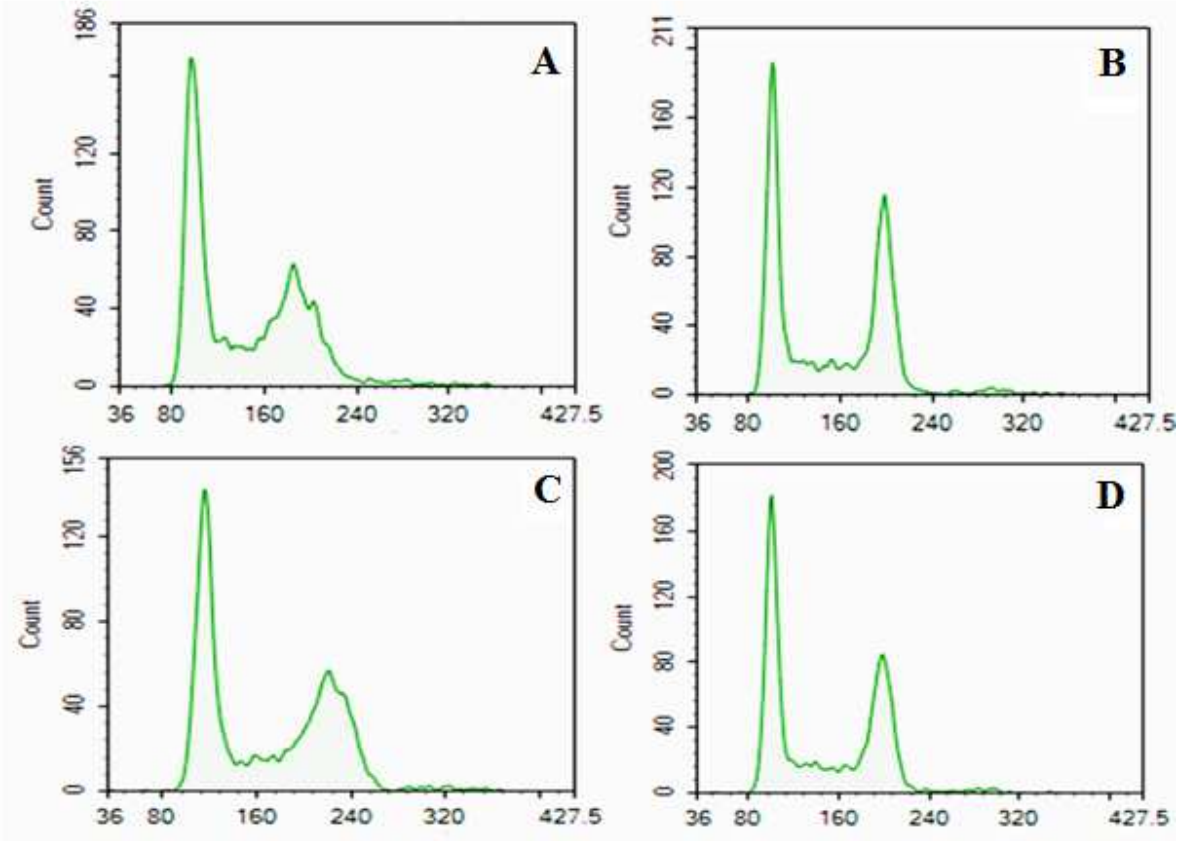

Fig. 4. Flow cytometry histograms showing the effect of compound **12c** on cell cycle distribution after 24 h treatment in MCF-7 cells. X-axis: DNA content of 20,000 events, y axis: cell number. A; 0µM; B: 5µM; C: 10µM; D: 20µM. The distribution of the different phases was analysed using the cell cycle algorithm of the NovoExpress software and the results expressed in Table 2.

Table 3: Cell cycle analysis of compound 13b. The distribution of the different phases was analysed using the cell cycle algorithm of the Novo Express software and expressed as percentage of total gated single events.

Stage	Concentration			
	Control	5 µM	10 µM	20 µM
Sub-G1	0.31%	0.40%	0.41%	0.91%
G1	33.41%	33.16%	34.52%	20.51%
S	24.95%	30.00%	26.36%	31.20%
G2-M	35.02%	31.39%	34.60%	44.87%

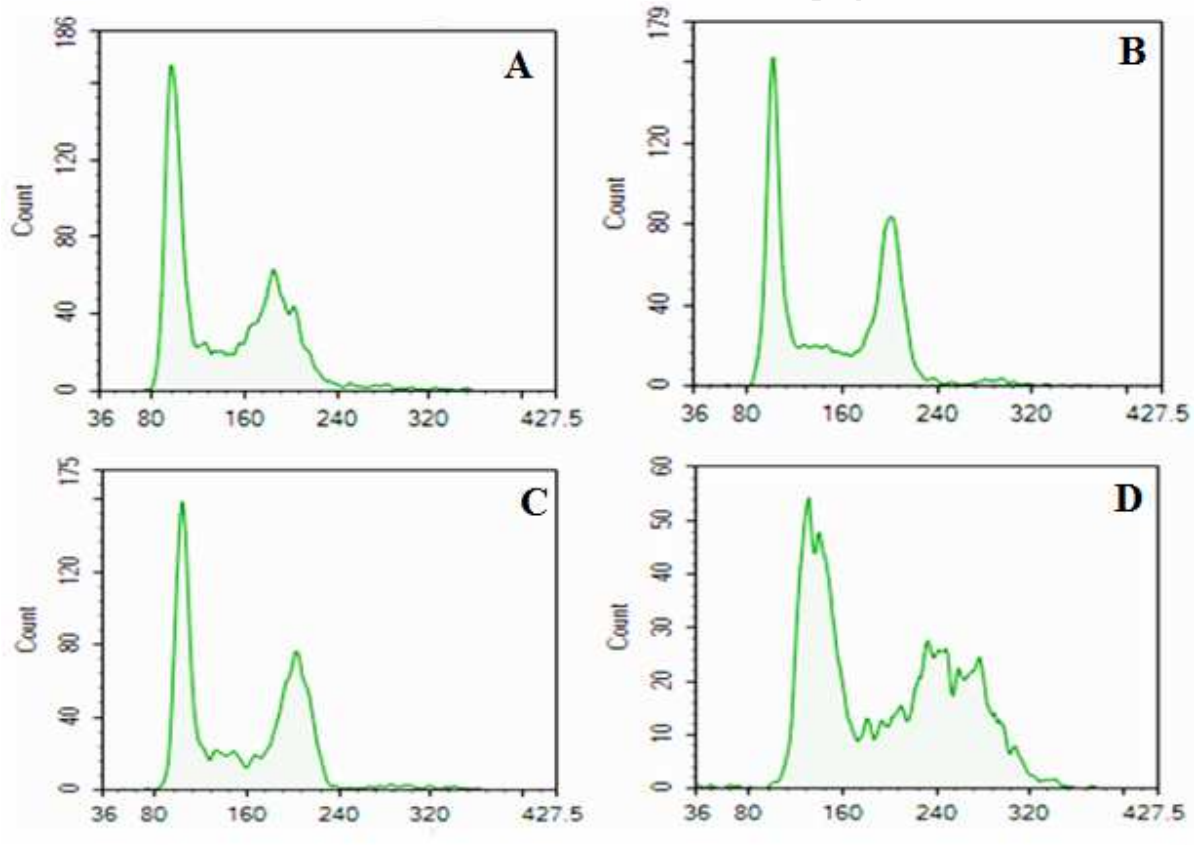

Fig. 5. Flow cytometry histograms showing the effect of compound **13b** on cell cycle distribution after 24 h treatment in MCF-7 cells. X-axis: DNA content of 20,000 events, y axis: cell number. A; 0µM; B: 5µM; C: 10µM; D: 20µM. The distribution of the different phases was analysed using the cell cycle algorithm of the Novo Express software and the results expressed in Table 2.

2.3.3. Annexin V FITC/PI apoptosis assay

The target compounds were designed based on merging the chemical structure of the apoptosis inducers **1-4**.Accordingly, compounds **12c** and **13b** were observed to have the highest activity against the three cancer cell lines (MCF-7, A2780, HT29), and were therefore selected, representing the two newly synthesized series, for further investigations to identify their mechanisms of action. The Annexin V Fluorescein Isothiocyanate/Propidium Iodide (FITC/PI) FITC/PI assay was used to evaluate their ability to induce apoptosis. For this,MCF-7 cells were treated with compound **12c** and **13b** for 24 h. The cells were then double stained with both Annexin V-FITC and PI, followed by analysis using flow cytometry (Beckman Coulter FC500 flow cytometer) to detect apoptosis using a method as previously described [40].Each of the compounds **12c** and **13b** increased the early apoptotic MCF-7 cell populations in a dose dependent manner (two and three fold, respectively, compared to control) (Fig. 6 and 7). Data analysis to determine the different phases of apoptosis was carried out using the Expo 32 software.

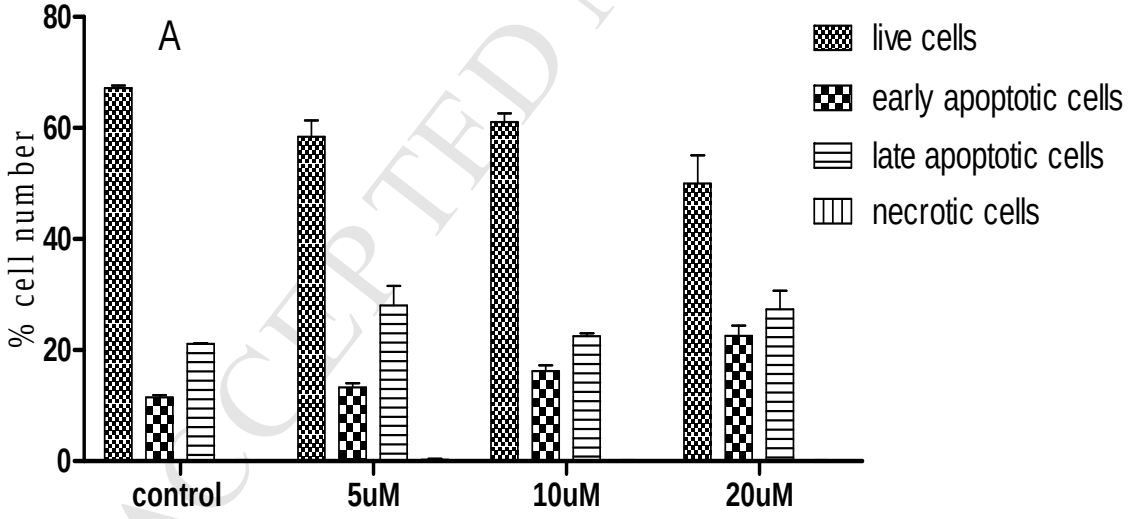

Fig. 6. Apoptotic responses of MCF7 cells to 24h treatment with compound **12c**, using annexin V-FITC/PI dual staining. Live cells: PI-/annexin V- ; Early apoptotic cells: PI-/ annexin V+; Late apoptotic cells: PI+/ annexin V+; Necrotic cells: PI+/ annexin V-. Data shown is mean % cell number ± SD (n=2).

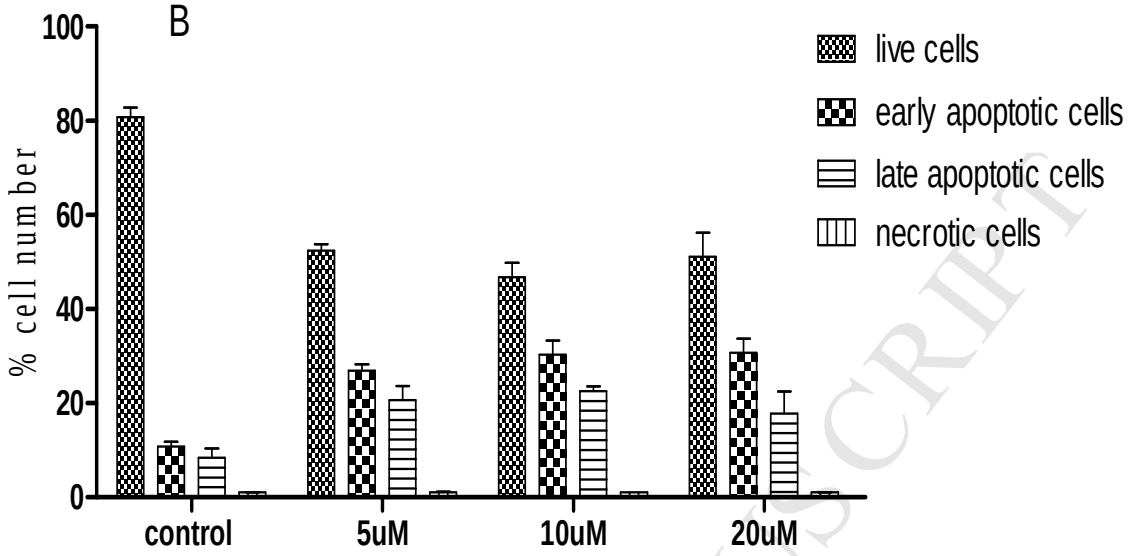

Fig.7. Apoptotic responses of MCF7 cells to 24h treatment with compound **13b**, using annexin V-FITC/PI dual staining. Live cells: PI-/annexin V- ; Early apoptotic cells: PI-/ annexin V+; Late apoptotic cells: PI+/ annexin V+; Necrotic cells: PI+/ annexin V-. Data shown is mean % cell number ± SD (n=2)

3. Conclusion

Two new series including Schiff bases of pyrrolizine-5-carboxamide and their Cu(II) complexes were synthesized and analyzed using spectral and elemental analysis. The cytotoxic activity of the new compounds was evaluated against the cancer cell linesMCF-7 (human breast adenocarcinoma), A2780 (human ovarian adenocarcinoma) and HT29 (human colon adenocarcinoma) in this study. The responses observed were compared to normal human fetal lung fibroblasts (MRC5), and the tested compounds showed IC_{50} values in the range of 0.04-24.66 µM. Compounds **12c** and **13b** were the most active in the two series, with IC_{50} values in the sub-micromolar range against MCF-7 and A2780 cancer cells. Compound **12c** showed high selectivity (6-13 fold) for the three cell lines over MRC5 normal cells. Furthermore, compound **12c**, induced an increase in the G1 and S cell cycle phases of MCF-7 cells after cell cycle analysis. In contrast, compound **13b** increased MCF-7 sub-G1 pro-apoptotic populations, and blocked cells in the G2-M phase in a dose dependent manner, at the expense of a decrease in G1.

Moreover, using the Annexin V apoptosis assay, compounds **12c** and **13b** were shown to increase the early apoptotic MCF-7 cell populations in a dose dependent manner (two and three fold, respectively).As such, the two compounds could be promising cytotoxic drug candidates, and warrant further *in vitro* and *in vivo* studies.

4. Experimental

4.1. Chemistry

Chemical reagents and solvents were purchased from Sigma-Aldrich. Thin-layer chromatography (TLC) was used to follow-up the reactions and to check the purity of the compounds. Melting points (m.p.) are uncorrected and were determined by digital melting point apparatus (IA 9100MK). A BRUKER TENSOR 37 spectrophotometer was used to determine the Infrared spectra (IR) using KBr disc. The IR spectra were expressed in wave number (cm^{-1}). The proton magnetic spectra were recorded on a BRUKER AVANCE III at 500 MHz (faculty of pharmacy, Umm Al-Qura University, KSA) in chloroform, and *j* constants are given in Hz. The ^{13}C-NMR spectra of the new compounds in chloroform were done at 125 MHz. The electron impact mass spectral data have been measured by a Finnigan MAT8222 instrument at 70 eV. Elemental analyses were done in the microanalytical center, Cairo University. Shimadzu TG-50 thermogravimetric analyzer was used to study the thermal behavior (TGA) of the solid chelates within 25-800 $^{\circ}$C range; heating rate 10°Cmin^{-1} under inert atmosphere. Compounds **8**, **10a-e** and **11a-e** were prepared according to previous reports [20-22].

*4.2. General procedure for the preparation of compounds **12a-e**.*

A mixture of compounds **11a-e** (2 mmol), cinnamaldehyde (2.2 mmol) and glacial acetic acid (0.5 ml) in absolute ethanol (30 mL) was refluxed for six hours. The solvent was evaporated under reduced pressure and crude product was recrystallized from chloroform-acetone (1:1).

*4.2.1. 7-Cyano-N-phenyl-6-((3-phenylallylidene)amino)-2,3-dihydro-1H-pyrrolizine-5-carboxamide **(12a).***

Compound **11a** was refluxed with cinnamaldehyde to generate compound **12a** as yellow crystals, m.p. 245-8 °C, yield 66%. IR (cm^{-1}, KBr phase): 3270 (ν_{NH}), 3030 (ν_{Ar-H}), 2210

($\nu_{C\equiv N}$), 1616 ($\nu_{C=O}$), 1600 ($\nu_{C=N}$). ^{1}H-NMR ($CDCl_3$-500 MHz) δ (ppm): 2.48-2.54 (m, 2H, pyrrolizine CH_2-2), 2.95 (t, 2H, *J* = 7.6 Hz, pyrrolizine CH_2-1), 4.49 (t, 2H, *J* = 7.2 Hz, pyrrolizine CH_2-3), 7.11-7.18 (m, 2H, Ph-CH=CH), 7.33-7.39 (m, 3H, aromatic CH-3″+CH-4″+CH-5″), 7.43-7.46 (m, 3H, aromatic CH-3′+ CH-4′+ CH-5′), 7.59 (d, 2H, *J* = 7.1 Hz, aromatic CH-2″+ CH-6″), 7.70 (d, 2H, *J* = 8.0 Hz, aromatic CH-2′+ CH-6′), 8.91 (d, H, *J* = 9.0 Hz, N=CH), 10.81 (s, H, CONH). ^{13}C-NMR ($CDCl_3$-100 MHz) δ (ppm):24.46 (CH_2-2), 25.37 (CH_2-1), 50.12 (CH_2-N), 116.18, 117.92 (C≡N), 119.85, 123.93, 126.76, 128.24, 129.05, 129.09, 130.67, 135.01, 137.89, 138.43, 147.93, 148.30, 152.81, 158.20 (N=C), 161.25 (C=O). DEPT135 ($CDCl_3$-100 MHz) δ (ppm): 24.46, 25.37, 50.12, 119.84, 123.93, 126.77, 128.23, 129.05, 129.08, 130.66, 147.92.MS (EI): m/z (%) 381 (M^++1, 27), 380 (M^+, 100), 287 (61), 277 (19), 260 (67), 250 (67), 184 (14), 130 (11), 115 (24), 103 (8) 91 (5), 77 (15). Anal. Calcd. for $C_{24}H_{20}N_4O$ (380.44):C, 75.77; H, 5.30; N, 14.73. Found: C, 76.07; H, 5.36; N, 14.37.

*4.2.2. 7-Cyano-6-((3-phenylallylidene)amino)-N-(p-tolyl)-2,3-dihydro-1H-pyrrolizine-5-carboxamide **(12b)**.*

Compound **11b** was refluxed with cinnamaldehyde to generate compound **12b** as yellow crystals, m.p. 256-9 °C, yield 71%. IR (cm^{-1}, KBr phase): 3268 (ν_{NH}), 2998 (ν_{Ar-H}), 2214 ($\nu_{C\equiv N}$), 1664 ($\nu_{C=O}$), 1608 ($\nu_{C=N}$). ^{1}H-NMR ($CDCl_3$-500 MHz) δ (ppm): 2.34 (s, 3H, CH_3), 2.43-2.49 (m, 2H, *J* = 8.1 Hz, pyrrolizine CH_2-2), 2.87 (t, 2H, *J* = 7.6 Hz, pyrrolizine CH_2-1), 4.44 (t, 2H, *J* = 7.1 Hz, pyrrolizine CH_2-3), 7.05-7.10 (dd,H, *J* = 15.1, 9.9 Hz, Ph-CH=CH), 7.16 (d, 2H, *J* = 8.1 Hz, aromatic CH-3′+CH-5′), 7.24 (d, H, *J* = 16.0 Hz, aromatic Ph-CH), 7.42-7.45 (m, 3H, aromatic CH-3″+CH-4″+CH-5″), 7.54-7.57 (m, 4H, aromatic CH-2′+CH-6′+ CH-2″+ CH-6″), 8.88 (d, H, *J* = 8.9 Hz, N=CH), 10.71 (s, H, CONH). ^{13}C-NMR ($CDCl_3$-100 MHz) δ (ppm):20.94 (CH_3), 24.34 (CH_2-2), 25.28 (CH_2-1), 50.06 (CH_2-N), 116.40, 117.88(C≡N),, 119.51, 119.61, 127.18, 128.09, 129.01, 129.54, 130.36, 133.34, 135.13, 135.95, 138.32, 146.93, 148.26, 158.07 (N=C),, 160.59 (C=O). DEPT135 ($CDCl_3$-100 MHz) δ (ppm): 20.94, 24.34, 25.28, 50.06, 119.61, 127.19, 128.09, 129.01, 129.54, 130.35, 146.92.MS (EI): m/z (%) 395 (M^++1, 27), 394 (M^+, 100), 287 (69), 260 (88), 184 (23), 130 (13), 115 (35), 103 (12), 91 (9), 77 (21). Anal. Calcd. for $C_{25}H_{22}N_4O$ (394.47):C, 76.12; H, 5.62; N, 14.20. Found: C, 75.89; H, 5.66; N, 14.38.

*4.2.3. 7-Cyano-N-(4-methoxyphenyl)-6-((3-phenylallylidene)amino)-2,3-dihydro-1H-pyrrolizine-5-carboxamide **(12c)**.*

Compound **11c** was refluxed with cinnamaldehyde to generate compound **12c** as yellow crystals, m.p. 225-7 °C, yield 73%. IR (cm^{-1}, KBr phase): 3273 (ν_{NH}), 2932 (ν_{Ar-H}), 2209 ($\nu_{C\equiv N}$), 1671 ($\nu_{C=O}$), 1578 ($\nu_{C=N}$). ^{1}H-NMR ($CDCl_3$-500 MHz) δ (ppm):2.39-2.45 (m, 2H, pyrrolizine CH_2-2), 2.82 (t, 2H, J = 7.2 Hz, pyrrolizine CH_2-1), 3.79 (s, 3H, OCH_3), 4.39-4.41 (t, 2H, J = 6.9 Hz, pyrrolizine CH_2-3), 6.88 (d, 2H, J = 8.3 Hz, aromatic CH-3′+CH-5′), 7.00-7.05 (dd, H, Ph-CH=C<u>H</u>), 7.18 (d, H, J = 15.8 Hz, Ph-C<u>H</u>), 7.39-7.41 (m, 3H, aromatic CH-3″+CH-4″+CH-5″), 7.51 (d, 2H, aromatic CH-2′+CH-6′), 7.57-7.59 (d, 2H, aromatic CH-2″+CH-6″), 8.85 (d, H, J = 8.8 Hz, N=CH), 10.63 (s, H, CONH). ^{13}C-NMR ($CDCl_3$-100 MHz) δ (ppm): 24.27 (CH_2-2), 25.22 (CH_2-1), 50.03 (CH_2-N), 55.47 (OCH_3), 114.19, 116.49, 117.79 (C≡N),, 120.90, 121.00, 127.30, 128.03, 128.98, 130.24, 131.80, 135.15, 138.43, 146.58, 148.23, 155.96, 157.92 (N=C), 160.31 (C=O). DEPT135 ($CDCl_3$-100 MHz) δ (ppm): 24.28, 25.23, 50.04, 55.48, 114.20, 120.91, 121.00, 127.31, 128.04, 128.99, 130.26, 146.59.MS (EI): m/z (%) 411 (M^++1, 29), 410 (M^+, 100), 307 (16), 287 (36), 260 (81), 232 (11), 205 (9), 184 (17), 130 (8), 115 (29), 103 (8), 88 (14). Anal. Calcd. for $C_{25}H_{22}N_4O_2$ (410.47): C, 73.15; H, 5.40; N, 13.65. Found: C, 73.22; H, 5.44; N, 14.09.

*4.2.4. N-(4-Chlorophenyl)-7-cyano-6-((3-phenylallylidene)amino)-2,3-dihydro-1H-pyrrolizine-5-carboxamide **(12d)***

Compound **11d** was refluxed with cinnamaldehyde to generate compound **12d** as yellow crystals, m.p. 253-5 °C, yield 64%. IR (cm^{-1}, KBr phase): 3278 (ν_{NH}), 2996 (ν_{Ar-H}), 2210 ($\nu_{C\equiv N}$), 1637 ($\nu_{C=O}$), 1610 ($\nu_{C=N}$),^{1}H-NMR ($CDCl_3$-500 MHz) δ (ppm):2.53-2.59 (m, 2H, pyrrolizine CH_2-2), 3.02 (t, 2H, J = 7.4 Hz, pyrrolizine CH_2-1), 4.49 (t, 2H, J = 7.2 Hz, pyrrolizine CH_2-3), 7.22-7.25 (dd, H, Ph-CH=C<u>H</u>), 7.33 (d, 2H, J = 8.6 Hz, aromatic CH-3′+CH-5′), 7.41-7.47 (m, 4H, Ph-C<u>H</u> + aromatic CH-3″+CH-4″+CH-5″), 7.61 (broad s, 2H, aromatic CH-2″+CH-6″), 7.68 (d, 2H, J = 8.8 Hz, aromatic CH-2′+ CH-6′), 8.88 (d, H, J = 8.9 Hz, N=CH), 10.88 (s, H, CONH).^{13}C-NMR ($CDCl_3$-100 MHz) δ (ppm): 24.58 (CH_2-2), 25.43(CH_2-1), 50.16 (CH_2-N), 115.78, 117.86(C≡N), 121.18, 125.94, 128.51, 128.86, 129.00, 129.18, 131.19, 134.76, 136.98, 148.36, 149.58, 152.81, 158.01 (N=C),, 162.14 (C=O). DEPT135 ($CDCl_3$-100 MHz) δ (ppm): 24.58, 25.43, 50.16, 121.18, 125.95, 128.50,

129.00, 129.18, 131.19, 149.56. MS (EI): m/z (%) 416 (M^++2, 36), 415 (M^++1, 44), 414 (M^+, 100), 311 (13), 287 (73), 260 (96), 184 (13), 130 (12), 115 (27), 103 (9), 91 (5), 77 (11). Anal. Calcd. for $C_{24}H_{19}ClN_4O$ (414.89):C, 69.48; H, 4.62; N, 13.50. Found: C, 70.17; H, 4.48; N, 13.67.

*4.2.5. N-(4-Bromophenyl)-7-cyano-6-((3-phenylallylidene)amino)-2,3-dihydro-1H-pyrrolizine-5-carboxamide **(12e).***

Compound **11e** was refluxed with cinnamaldehyde to generate compound **12e** as yellow crystals, m.p. 253-6 °C, yield 75%. IR (cm^{-1}, KBr phase): 3226 (ν_{NH}), 2988 (ν_{Ar-H}), 2210 ($\nu_{C\equiv N}$), 1673 ($\nu_{C=O}$), 1578 ($\nu_{C=N}$). ^{1}H-NMR ($CDCl_3$-500 MHz) δ (ppm):2.50-2.55 (m, 2H, pyrrolizine CH_2-2), 2.97 (t, 2H, J = 7.4 Hz, pyrrolizine CH_2-1), 4.46 (t, 2H, J = 7.0 Hz, pyrrolizine CH_2-3), 7.09 (dd,H, Ph-CH=C<u>H</u>), 7.33 (d, H, J = 15.8 Hz, Ph-C<u>H</u>), 7.45-7.47 (m, 5H, aromatic CH-3′+CH-5′+CH-3″+CH-4″+CH-5″), 7.57-7.60 (m, 4H, aromatic CH-2′+CH-6′+CH-2″+CH-6″), 8.90 (d, H, J = 9.1 Hz, N=CH), 10.86 (s, H, CONH). ^{13}C-NMR ($CDCl_3$-100 MHz) δ (ppm): 24.49(CH_2-2), 25.35(CH_2-1), 50.11(CH_2-N), 116.08, 116.29, 117.67(C≡N), 121.25, 126.68, 128.21, 129.11, 130.74, 131.96, 134.93, 137.57, 138.18, 148.04, 148.46, 152.79, 158.16(N=C), 161.28 (C=O). DEPT135 ($CDCl_3$-100 MHz) δ (ppm): 24.49, 25.35, 50.11, 121.24, 126.71, 128.21, 129.11, 130.73, 131.96, 147.98.MS (EI): m/z (%) 460 (M^++2, 71), 459 (M^++1, 55), 458 (M^+, 72), 355 (12), 328 (12), 287 (85), 260 (100), 232 (12), 184 (16), 130 (14), 115 (29), 103 (10),91 (11), 77 (12). Anal. Calcd. for $C_{24}H_{19}BrN_4O$ (459.34):C, 62.75; H, 4.17; N, 12.20. Found: C, 63.47; H, 4.27; N, 12.87.

*4.3. General procedure for preparation of compounds **13a-e***

Copper(II) chloride dihydrate (2mmol; 0.34 g) andpyrrolizine-5-carboxamides ligands (**12a-e**) (2mol; 0.76 g of **12a**, 0.78 g of **12b**, 0.82 g of **12c**, 0.83 g of **12d** and 0.92 g of **12e**) were refluxed in dry acetonitrile (50 mL) for 10 h. The deep brown complexes formed on heat were filtered off and washed with hot acetonitrile. The crude product was dried and recrystallized from acetonitrile.

*4.3.1. $[Cu(L^{12a})_2(H_2O)_2].CH_3CN$ **(13a).***

Yield 54 %, deep brown solid, m.p.229-31°C; Anal. Calcd. for $C_{50}H_{45}N_9O_4Cu$ (899.5):C, 66.76; H, 5.04; N, 14.01, Cu, 7.06. Found: C, 67.27; H, 4.57; N, 14.47, Cu, 6.90.Λ_m (/Ω^{-1}

cm^2mol^{-1})= 12.2;IR (cm^{-1}, KBr phase): 3449 (ν_{H2O}), 3030 (ν_{Ar-H}), 2212 ($\nu_{C\equiv N}$), 1694 ($\nu_{C=N}$), 1579 ($\nu_{C=N}$), 594 (ν_{Cu-O}), 480 (ν_{Cu-N})

4.3.2. [$CuL^{12b}Cl_2$] ***(13b)***

Yield 60 %, deep brown solid, m.p.343-5°C; Anal. Calcd. for $C_{25}H_{22}N_4OCuCl_2$ (528.92): C, 56.77; H, 4.19; N, 10.59, Cu, 12.01. Found: C, 56.07; H, 4.33; N, 10.89; Cu, 11.89.Λ_m ($/\Omega^{-1}$ cm^2 mol^{-1})= 16.8;IR (cm^{-1}, KBr phase) 3235 (ν_{NH}), 2975 (ν_{Ar-H}), 2218 ($\nu_{C\equiv N}$), 1694 ($\nu_{C=O}$), 1601 ($\nu_{C=N}$), 520 (ν_{Cu-O}), 491 (ν_{Cu-N}).

4.3.3. [$Cu(L^{12c})_2$] ***(13c)***

Yield 58 %, deep brown solid, m.p.334-7°C; Anal. Calcd. for $C_{50}H_{42}N_8O_4Cu$ (882.47): C, 68.05; H, 4.80; N, 12.70; Cu, 7.20. Found: C, 68.67; H, 4. 73; N, 13.47;Cu, 7.91; Λ_m ($/\Omega^{-1}$ cm^2 mol^{-1})= 13.9;IR (cm^{-1}, KBr phase): 2931 (ν_{Ar-H}), 2223 ($\nu_{C\equiv N}$), 1689 ($\nu_{C=N}$), 1607 ($\nu_{C=N}$), 590 (ν_{Cu-O}), 494 (ν_{Cu-N})

4.3.4.[$CuL^{12d}Cl_2$] ***(13d)***

Yield 60 %, deep brown solid, m.p.247-9°C; Anal. Calcd. for $C_{24}H_{19}N_4OCuCl_3$ (549.34): C, 52.47; H, 3.49; N, 10.20; Cu, 11.57. Found: C, 52.19; H, 4.46; N, 11.76, Cu, 11.50; Λ_m ($/\Omega^{-1}$ cm^2 mol^{-1})= 15.3;IR (cm^{-1}, KBr phase): 3281 (ν_{NH}), 2997 (ν_{Ar-H}), 2211 ($\nu_{C\equiv N}$), 1646 ($\nu_{C=O}$), 1619 ($\nu_{C=N}$), 573 (ν_{Cu-O}), 481 (ν_{Cu-N}).

4.3.5.[$CuL^{12e}Cl_2$ $(CH_3CN)_2$].H_2O ***(13e)***.

Yield 60 %, deep brown solid, m.p .> 350°C; Anal. Calcd. for $C_{28}H_{27}N_6O_2CuCl_2Br$ (693.91): C, 48.46; H, 3.92; N, 12.11; Cu, 9.16. Found: C, 48.43; H, 3.66; N, 11.96; Cu, 9.28; Λ_m ($/\Omega^{-1}$ cm^2 mol^{-1})= 14.8; IR (cm^{-1}, KBr phase): 3447 (ν_{H2O}), 3339 (ν_{NH}), 2977 (ν_{Ar-H}), 2219 ($\nu_{C\equiv N}$), 1661 ($\nu_{C=O}$), 1601 ($\nu_{C=N}$), 593 (ν_{Cu-O}), 476 (ν_{Cu-N})

4.4. Pharmacological screening

4.4.1. Growth inhibition

4.4.1.1. Cell culture

Three cancer adenocarcinoma cell lines, MCF-7 (human breast adenocarcinoma), A2780 (human ovarian adenocarcinoma) and HT29 (human colon) adenocarcinoma), were used in this study. For comparison of cancer cell responses compared to normal cells, the MRC5 normal human

fetal lung fibroblast cell line was also used. All cell lines were obtained from the ATCC. The three cancer cells were sub-cultured in RPMI-1640 media (supplemented with 10% FBS); while MRC5 was maintained in Eagles minimum essential medium (EMEM, supplemented with 10% FBS); growth was maintained in a 37°C incubator in a mixture of 5% CO_2 and air, with a relative humidity of 100%.

4.4.1.2. Cytotoxicity assay

As previously reported [38], the cytotoxicity of the new compounds was evaluated by the MTT assay. The three cancer cell lines (MCF-7, A2780, HT29) and the normal fibroblasts (MRC5) were separately cultured in 96-well plates (3 $\times 10^3$/well), and incubated at 37 °C overnight. Final compound concentrations: 0, 0.05, 0.5, 5, 25, 50 μM (DMSO 0.1%; n= 3). The plates were incubated with the compounds for 72 h, followed by addition of MTT to each well. The plates were incubated for a further 3 hr, supernatant was aspirated, and DMSO added to each well. Absorbance was read on a multi-plate reader, with the optical density of the purple formazan A_{550} being proportional to the number of viable cells. Compound concentration causing 50% inhibition (IC_{50}) compared to control cell growth (100%) was determined. Graph Pad Prism version 5.00 for Windows was used for analysis (Graph Pad Software, San Diego, California, USA).

4.4.2. Determination of cell cycle perturbations

To determine any effects of the new compounds on the cell cycle, distribution analysis was done according to the previous method [39]. MCF-7 cells were cultured in 6 well plates (1×105 cells) overnight at 37 °C. The cells were then treated with either compound **12c** or **13b** (0, 5, 10 and 20 μM) for 24h, followed by washing with PBS. After trypsinsation, cells were collected and then centrifuged at 400 xg, following which the resulting pellets were washed in cold PBS. After another spin, the cells were fixed overnight in 70% ice cold ethanol. Following centrifugation to remove the ethanol, cells were re-suspended in cold PBS and ribonuclease A added for 15 min, which was then followed by the addition of PI (2 μl/ml). Samples were held on ice, and analysed by flow cytometry using the Novo Cyte flow cytometer. Data analysis was done, using the Novo Express cell cycle algorithm, comparing the DNA contents (PI bound to DNA) of 20000 events.

Doublets were differentiated from single cells in the G_2-M phase by gating them out manually.The results were presented in Fig. 5.

4.4.3. Annexin V FITC/PI apoptosis assay

Apoptosis using Annexin V FITC/PI staining according to the previous report [40]. MCF-7 cells were cultured in 6 well plates (1×10^5 cells/well) overnight at 37 °C. Each of compound **12c** and **13b** were used to treat cells (0, 5, 10 and 20 µM). After 24 h, supernatants of the treated cells were collected in tubes and kept on ice. Consequently, cells were trypsinized, before being added to the tubes, and then centrifuged (500 xg). After a further wash with PBS, the cells were centrifuged again, and pellets re-suspended in annexin V binding buffer (100 µL) and annexin V FITC (10 µL). Tubes were incubated at room temperature in dark for 20 min, before adding binding buffer (400 µL,) and 10 µL propidium iodide (PI). Analysis was performed by flow cytometry (Beckman Coulter Flow Cytometer, Texas, USA). Different cell populations (early apoptotic, late apoptotic, and necrotic cells) were identified using annexin V and PI staining.

Supplementary data

Supplementary data including all spectral data and copies of IR, ^{1}H-NMR, ^{13}C-NMR, Mass, thermal and ESR spectra, of all the final compounds were provided with this manuscript (Figures S1-S30).

Conflict of Interest

All authors of this manuscript have not declared any conflict of interest.

References

1. WHO, Fact sheet (accessed in 7-9-2017), http://www.who.int/mediacentre/factsheets/fs297/en/.
2. W.C. Huang, Y.J. Chen, M.C. Hung, Implication of nuclear EGFR in the development of resistance to anticancer therapies, Biomed. 1 (2011) 2–10. doi:10.1016/j.biomed.2011.10.001.
3. A. Persidis, Cancer multidrug resistance, Nat. Biotechnol. 17 (1999) 94–95. doi:10.1038/80051.

4. J.A. Hickman, Apoptosis induced by anticancer drugs, Cancer Metastasis Rev. 11 (1992) 121–139.
5. S. Fulda, Targeting apoptosis for anticancer therapy, Semin. Cancer Biol. 31 (2015) 84–88. doi:10.1016/j.semcancer.2014.05.002.
6. A.M. Gouda, A.H. Abdelazeem, An integrated overview on pyrrolizines as potential anti-inflammatory, analgesic and antipyretic agents, Eur. J. Med. Chem. 114 (2016) 257–292. doi:10.1016/j.ejmech.2016.01.055.
7. S.E. Abbas, F.M. Awadallah, N.A. Ibrahim, A.M. Gouda, B.A. Shehata, Design, synthesis and preliminary evaluation of some novel [1,4]diazepino[5,6-b]pyrrolizine and 6-(2-oxopyrrolidino)-1H-pyrrolizine derivatives as anticonvulsant agents, Med. Chem. Res. 20 (2011) 1015–1023. doi:10.1007/s00044-010-9429-8.
8. A. Gouda, H. Ali, W. Almalki, M. Azim, M. Abourehab, A. Abdelazeem, Design, Synthesis, and Biological Evaluation of Some Novel Pyrrolizine Derivatives as COX Inhibitors with Anti-Inflammatory/Analgesic Activities and Low Ulcerogenic Liability, Molecules 21 (2016) 201. doi:10.3390/molecules21020201.
9. W. Liu, J. Zhou, K. Bensdorf, H. Zhang, H. Liu, Y. Wang, H. Qian, Y. Zhang, A. Wellner, G. Rubner, W. Huang, C. Guo, R. Gust, Investigations on cytotoxicity and anti-inflammatory potency of licofelone derivatives, Eur. J. Med. Chem. 46 (2011) 907–913. doi:10.1016/j.ejmech.2011.01.002.
10. S. Tavolari, M. Bonafè, M. Marini, C. Ferreri, G. Bartolini, E. Brighenti, S. Manara, V. Tomasi, S. Laufer, T. Guarnieri, Licofelone, a dual COX/5-LOX inhibitor, induces apoptosis in HCA-7 colon cancer cells through the mitochondrial pathway independently from its ability to affect the arachidonic acid cascade, Carcinogenesis 29 (2008) 371–380. doi:10.1093/carcin/bgm265.
11. N.K. Narayanan, D. Nargi, M. Attur, S.B. Abramson, B.A. Narayanan, Anticancer effects of licofelone (ML-3000) in prostate cancer cells, Anticancer Res. 27 (2007) 2393–2402.
12. A.M. Gouda, A.H. Abdelazeem, E.-S.A. Arafa, K.R.A. Abdellatif, Design, synthesis and pharmacological evaluation of novel pyrrolizine derivatives as potential anticancer agents, Bioorg. Chem. 53 (2014) 1–7. doi:10.1016/j.bioorg.2014.01.001.

13. A.M. Gouda, A.H. Abdelazeem, H.A. Omar, A.N. Abdalla, M.A.S. Abourehab, H.I. Ali, Pyrrolizines: design, synthesis, anticancer evaluation and investigation of the potential mechanism of action, Bioorg. Med. Chem. (n.d.). doi: 10.1016/j.bmc.2017.08.039.
14. H. Ka, H.-J. Park, H.-J. Jung, J.-W. Choi, K.-S. Cho, J. Ha, K.-T. Lee, Cinnamaldehyde induces apoptosis by ROS-mediated mitochondrial permeability transition in human promyelocytic leukemia HL-60 cells, Cancer Lett. 196 (2003) 143–152. doi:10.1016/S0304-3835(03)00238-6.
15. H.W. Jeong, D.C. Han, K.H. Son, M.Y. Han, J.S. Lim, J.H. Ha, C.W. Lee, H.M. Kim, H.C. Kim, B.M. Kwon, Antitumor effect of the cinnamaldehyde derivative CB403 through the arrest of cell cycle progression in the G2/M phase, Biochem. Pharmacol. 65 (2003) 1343–1350. doi:10.1016/S0006-2952(03)00038-8.
16. S.Y. Shin, H. Jung, S. Ahn, D. Hwang, H. Yoon, J. Hyun, Y. Yong, H.J. Cho, D. Koh, Y.H. Lee, Y. Lim, Polyphenols bearing cinnamaldehyde scaffold showing cell growth inhibitory effects on the cisplatin-resistant A2780/Cis ovarian cancer cells, Bioorganic Med. Chem. 22 (2014) 1809–1820. doi:10.1016/j.bmc.2014.01.058.
17. D. Montagner, V. Gandin, C. Marzano, A. Erxleben, DNA damage and induction of apoptosis in pancreatic cancer cells by a new dinuclearbis(triazacyclonane) copper complex, J. Inorg. Biochem. 145 (2015) 101–107. doi:10.1016/j.jinorgbio.2015.01.013.
18. M. Sutradhar, Rajeshwari, T. Roy Barman, A.R. Fernandes, F. Paradinha, C. Roma-Rodrigues, M.F.C. Guedes da Silva, A.J.L. Pombeiro, Mixed ligand aroylhydrazone and N-donor heterocyclic Lewis base Cu(II) complexes as potential antiproliferative agents, J. Inorg. Biochem. 175 (2017) 267–275. doi:10.1016/j.jinorgbio.2017.07.034.
19. C. Fernandes, A. Horn, B.F. Lopes, E.S. Bull, N.F.B. Azeredo, M.M. Kanashiro, F. V. Borges, A.J. Bortoluzzi, B. Szpoganicz, A.B. Pires, R.W.A. Franco, J.C.D.A. Almeida, L.L.F. Maciel, J.A.L.C. Resende, G. Schenk, Induction of apoptosis in leukemia cell lines by new copper(II) complexes containing naphthyl groups via interaction with death receptors, J. Inorg. Biochem. 153 (2015) 68–87. doi:10.1016/j.jinorgbio.2015.09.014.
20. A. Etienne, Y. Correia, Derivatives of 2-pyrrolidone, Bull. Soc. Chem. 10 (1969) 3704-3712.
21. W.A. Jacobs, M. Heidelberger, The ferrous sulfate and ammonia method for the reduction of nitro to amino compounds, J. Amer. Chem. Soc. 39 (1917)1435-1439.

22. M.Y. Ebeid, S.M. El-Moghazy, M.M. Hanna, F.A. Romeih and F.F. Barsoum, Synthesis and anti-HIV activity of some 6,7-dihydro-5*H*-pyrrolizine-3-carboxamide, 5,6,7,8-tetrahydroindolizine-3-carboxamide, 1-thioxo-1,2,3,5,6,7,8,9,10,11-decahydro-pyrimido-[1,6-a]azonine-4-carbo-nitrile and 6-thioxo-1,2,5,6,8,9,10,11,12,13,14,14a-dodecahydropyrimido [4', 5': 4, 5]pyrimido[1,6-a]azonine-1-one derivatives, Bull. Fac. Pharm. Cairo Univ. 35 (1997) 171–183.
23. W.J. Geary, The use of conductivity measurements in organic solvents for the characterization of coordination compounds, Coord. Chem. Rev. 7 (1971) 81–122. doi: 10.1016/S0010-8545(00)80009-0.
24. S.D. Joshi, D. Kumar, S.R. Dixit, N. Tigadi, U.A. More, C. Lherbet, T.M. Aminabhavi, K.S. Yang, Synthesis, characterization and antitubercular activities of novel pyrrolylhydrazones and their Cu-complexes, Eur. J. Med. Chem. 121 (2016) 21-39. doi: 10.1016/j.ejmech.2016.05.025.
25. A.H. Kianfar, S. Ramazani, R.H. Fath, M. Roushani, Synthesis, spectroscopy, electrochemistry and thermogravimetry of copper(II) tridentate Schiff base complexes, theoretical study of the structures of compounds and kinetic study of the tautomerism reactions by ab initio calculations, Spectrochim. Acta A 105 (2013) 374–382.doi: 10.1016/j.saa.2012.12.010.
26. N.H. Yarkandi, H.A. El-Ghamry, M. Gaber, Synthesis, spectroscopic and DNA binding ability of Co^{II}, Ni^{II}, Cu^{II} and Zn^{II} complexes of Schiff base ligand (E)-1-(((1H-benzo [d] imidazol-2-yl) methylimino) methyl) naphthalen-2-ol. X-ray crystal structure determination of cobalt (II) complex, Mat. Sci. Eng. C 75 (2017) 1059–1067.doi: 10.1016/j.msec.2017.02.171.
27. G.Q. Zhong, J. Shen, Q.Y. Jiang, Y.Q. Jia, M.J. Chen, Z.P. Zhang, Synthesis, characterization and thermal decomposition of Sb^{III}-M-Sb^{III} type trinuclear complexes of ethylenediamine-N,N,N′,N′-tetraacetate (M:Co(II), La(III), Nd(III), Dy(III)), J. Therm. Anal. Calorim. 92 (2008) 607–616. doi: 10.1007/s10973-007-8579-5.
28. J.R. Allan, W.C. Geddes, C.S. Hindle, A.E. Orr, Thermal analysis studies on pyridine carboxylic acid complexes of zinc(II), Thermochim. Acta C 153 (1989) 249-25. 10.1016/0040-6031(89)85438-3.

29. M. Badea, A. Emandi, D. Marinescu, E. Cristurean, R. Olar, A. Braileanu, P. Budrugeac, E. Segal, Thermal stability of some azo-derivatives and their complexes, J. Therm. Anal. Calorim. 72 (2003) 525. doi:10.1023/A:1024517430630
30. M.M. Al-Neaimi, M.M. Al-Khuder, Synthesis, characterization and extraction studies of some metal (II) complexes containing (hydrazoneoxime and bis-acylhydrazone) moieties, Spectrochim. Acta A 105 (2013) 365. doi: 10.1016/j.saa.2012.10.046.
31. K.Y. El-Baradie, N.A. El-Wakiel, H.A. El-Ghamry, Synthesis, characterization and corrosion inhibition in acid medium of L-histidine Schiff base complexes, Appl. Organometal. Chem. 29, 3 (2015) 117–125. doi: 10.1002/aoc.3255.
32. H. Liu, H. Wang, F. Gao, D. Niu, Z. Lu, Self-assembly of copper(II) complexes with substituted aroylhydrazones and monodentate N-heterocycles: synthesis, structure and properties, J. Coord. Chem. 60 (2007) 2671. doi: 10.1080/00958970701302404.
33. H.A. El-Ghamry, S. Masaoka, K. Sakai, Hydrogen-bonded frameworks of propylenediamine-N,N′-diacetic acid Pt(II) complexes, synthesis, structural characterization, and antitumor activity, J. coord. Chem. 67, 6 (2014) 943-955. doi: 10.1080/00958972.2014.900550.
34. J.V. Mehta, S.B. Gajera, D.D. Patel, M.N. Patel, Synthesis, spectral investigation and development of tetrahedral copper(II) complexes as artificial metallonucleases and antimalarial agents , Appl. Organometal. Chem. 29 (2015) 357–367.
35. Y.-M. Lee, B.-J. Kim, H.-J. Kim, S.-Y. Kim, S.K. Kang, S.-N. Choi, Crystal structures and spectroscopic properties of copper(II) pseudohalide complexes with two sparteine epimers, having a CuN4 chromophore, Polyhedron 28 (2009) 3060– 3064.
36. P. Bindu, M.R.P. Kurup, T.R. Satyakeerty, Epr, cyclic voltammetric and biological activities of copper(II) complexes of salicylaldehyde N(4)-substituted thiosemicarbazone and heterocyclic bases, Polyhedron 18 (1999) 321–331. doi: 10.1016/S0277-5387(98)00166-1
37. B.J. Hathaway, D.E. Billing, The electronic properties and stereochemistry of mono-nuclear complexes of the copper (II) ion, Coord. Chem. Rev. 5 (1970) 143. doi: 10.1016/S0010-8545(00)80135-6.

38. E.A. Arafa, A.H. Abdelazeem, H.H. Arab, H.A. Omar, OSU-CG5, a novel energy restriction mimetic agent, targets human colorectal cancer cells in vitro., Acta Pharmacol. Sin. 35 (2014) 394–400. doi:10.1038/aps.2013.183.
39. A. Aslam, S. Mittal, F. Koch, J.-C. Andrau, G.S. Winkler, The Ccr4-NOT deadenylase subunits CNOT7 and CNOT8 have overlapping roles and modulate cell proliferation., Mol. Biol. Cell. 20 (2009) 3840–3850. doi:10.1091/mbc.E09-02-0146.
40. I. Vermes, C. Haanen, H. Steffens-Nakken, C. Reutelingsperger, A novel assay for apoptosis. Flow cytometric detection of phosphatidylserine expression on early apoptotic cells using fluorescein labeled Annexin V., J. Immunol. Methods. 184 (1995) 39–51.

Highlights

- The antitumor activity of novel pyrrolizines and their Cu(II) complexes were evaluated.
- The tested compounds showed IC_{50} values in the range of 0.04-24.66 μM.
- The substituted methyl-Cu complex blocked MCF-7 in the G2-M phase of the cell cycle.
- The most active compounds increase the early apoptotic MCF-7 cell populations.